

Spontaneous and Triggered Vortices in Polariton Optical-Parametric-Oscillator Superfluids

F. M. Marchetti,^{1,*} M. H. Szymańska,^{2,†} C. Tejedor,¹ and D. M. Whittaker³

¹*Departamento de Física Teórica de la Materia Condensada, Universidad Autónoma de Madrid, Madrid 28049, Spain*

²*Department of Physics, University of Warwick, Coventry, CV4 7AL, United Kingdom*

³*Department of Physics and Astronomy, University of Sheffield, Sheffield, S3 7RH, United Kingdom*

(Received 26 March 2010; revised manuscript received 8 June 2010; published 4 August 2010)

We study nonequilibrium polariton superfluids in the optical-parametric-oscillator regime by using a Gross-Pitaevskii equation with pumping and decay. We identify a regime above the optical-parametric-oscillator threshold, where the system undergoes spontaneous symmetry breaking and is unstable towards vortex formation without any rotating drive. Stable vortex solutions differ from metastable ones; the latter can persist but can be triggered only externally. Both spontaneous and triggered vortices are characterized by a generalized healing length, specified by the optical-parametric-oscillator parameters only.

DOI: 10.1103/PhysRevLett.105.063902

PACS numbers: 42.65.Yj, 47.32.-y, 71.36.+c

Since the first observation of stimulated scattering [1], resonantly driven polariton microcavities have been the subject of intensive research. Significant advances have taken place towards a new generation of low threshold lasers and ultrafast optical amplifiers and switches. However, only very recently resonantly pumped polaritons have been shown to exhibit a new form of nonequilibrium superfluid behavior [2–4]. In the optical-parametric-oscillator (OPO) regime [5], polaritons are continuously injected into the pump state and, above a pump strength threshold, undergo coherent stimulated scattering into the signal and idler states. Superfluidity has been demonstrated as frictionless flow [2]. Moreover, metastability of quantum vortices and persistence of currents have been proven by using a pulsed Laguerre-Gauss (LG) beam [4]. Vorticity has been observed to be transferred into the OPO signal and to persist in the absence of the driving rotating probe.

The polaritonic system is intrinsically nonequilibrium: Continuous pumping is needed to balance the fast polariton decay, of the order of picoseconds, and maintain a steady state regime. In strong contrast with equilibrium superfluids, whose ground state is flowless, pump and decay lead to currents that carry polaritons from gain- to loss-dominated regions. As a result of the interplay between these currents and a confining potential, polaritons non-resonantly injected into a microcavity have been shown to become unstable to spontaneous formation of vortices [6,7] and vortex lattices [8]. For resonant excitation, currents arise in the OPO regime due to the simultaneous presence of a pump, signal, and idler emitting at different momenta (see Fig. 1). In this Letter, we identify a regime of the OPO, where even in the absence of disorder or trapping potentials the system undergoes spontaneous breaking of the system symmetry and becomes unstable towards the formation of a quantized vortex state with charge $m = \pm 1$. We show that these spontaneous stable vortex solutions are robust to noise and to any other external perturbation and, thus, should be experimentally observable. Spontaneous

stable vortices differ from metastable ones, which can be injected only externally into an otherwise stable symmetric state and whose persistence is due to the OPO superfluid properties [4]. The metastable vortex is a possible but not unique stable configuration of the system. We find that the shape and size of the metastable vortices are independent on the external probe. In addition, like in equilibrium superfluids, both stable and metastable vortices are characterized by a healing length which is determined by the parameters of the OPO system alone. Controlled creation of vortices in OPO has been recently achieved by a weak continuous probe [9]. Metastable vortices have been also recently discussed for nonresonantly pumped polariton condensates in Ref. [10].

Model.—We describe the OPO dynamics via Gross-Pitaevskii equations [11] for coupled cavity and exciton fields $\psi_{C,X}(\mathbf{r}, t)$ with pumping and decay [12] ($\hbar = 1$):

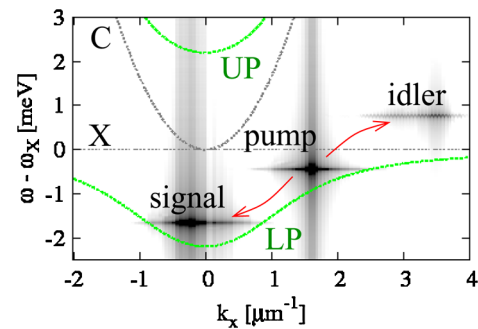


FIG. 1 (color online). OPO spectrum for a top-hat pump of FWHM $\sigma_p = 70 \mu\text{m}$ and intensity $f_p = 1.24f_p^{(\text{th})}$, where $f_p^{(\text{th})}$ is the threshold strength for OPO. Polaritons injected resonantly at $(k_p, 0)$ and ω_p undergo coherent stimulated scattering into the signal and idler states, which are blueshifted with respect to the bare LP dispersion (green dotted line) because of interactions. Cavity photon (C) and exciton (X) dispersions are plotted as gray dotted lines.

$$\begin{aligned}
i\partial_t \begin{pmatrix} \psi_X \\ \psi_C \end{pmatrix} &= \begin{pmatrix} 0 \\ F_p + F_{pb} \end{pmatrix} \\
&+ \begin{pmatrix} \omega_X - ik_X + g_X |\psi_X|^2 & \Omega_R/2 \\ \Omega_R/2 & \omega_C - ik_C \end{pmatrix} \\
&\times \begin{pmatrix} \psi_X \\ \psi_C \end{pmatrix}. \quad (1)
\end{aligned}$$

We neglect the exciton dispersion and assume a quadratic dispersion for photons, $\omega_C = \omega_C^0 - \frac{\nabla^2}{2m_C}$. The fields decay with rates $\kappa_{X,C}$, and Ω_R is the Rabi splitting. The cavity field is driven by a continuous wave pump, $F_p(\mathbf{r}, t) = \mathcal{F}_{f_p, \sigma_p}(r) e^{i(\mathbf{k}_p \cdot \mathbf{r} - \omega_p t)}$, where $\mathcal{F}_{f_p, \sigma_p}$ is either a Gaussian or a top-hat spatial profile with strength f_p and FWHM σ_p . The exciton interaction strength g_X can be set to one by rescaling both fields $\psi_{X,C}$ and pump strength F_p by $\sqrt{\Omega_R/(2g_X)}$. For the simulations shown in this Letter, $m_C = 2 \times 10^{-5} m_0$, the energy zero is fixed to $\omega_X = \omega_C^0$ (zero detuning), $\Omega_R = 4.4$ meV, and $\kappa_{X,C}$ are fixed so as to give a polariton lifetime of 3 ps.

For homogeneous pumps, the conditions under which a stable OPO switches on can be found analytically [13,14]. However, for a finite size pump, one has to resort to a numerical analysis [12]. Here, we solve Eq. (1) on a 2D grid by using both a 5th-order adaptive-step Runge-Kutta algorithm and the Crank-Nicholson method. Fixing the pump momentum $(k_p, 0)$ close to the lower polariton (LP) inflection point, we find the pump strength threshold f_p^{th} for which signal and idler states get exponentially populated. The OPO signal spatial profile $|\psi_{C,X}^s| e^{i\phi_{C,X}^s}$ can be obtained by filtering in a cone around the signal momentum at a given time. The photon component of the filtered OPO signal profile $|\psi_C^s|$ and its supercurrent $\nabla\phi_C^s$ are shown in the first left panel in Fig. 2. We select only OPO solutions which reach a steady state. Note that the pump direction $(k_p, 0)$ leaves the symmetry $y \mapsto -y$ intact. This symmetry, while allowing vortex-antivortex pairs, does not permit single vortices.

One can perform a dynamical stability analysis of the OPO by adding small fluctuations to the steady state mean field. Equivalently, stability can be checked numerically by introducing a weak noise. In particular, we add white noise as a quick pulse to both the modulus $|\psi_{X,C}(\mathbf{k}, t)|$ and phase $\phi_{X,C}(\mathbf{k}, t)$ of excitonic and photonic wave functions in momentum space. The noise added to the phase has amplitude 2π , and for the modulus we specify the noise strength in units of the maximum of the pump intensity in momentum space.

Stable vortex solutions.—Remarkably, we have singled out symmetric OPO states, as shown in the first row in Fig. 2, which are unstable towards the spontaneous formation of stable vortex solutions. Once the $y \mapsto -y$ symmetry is broken by the noise pulse of any strength, we have observed a vortex with quantized charge $m = \pm 1$ ($m = \mp 1$) entering and stabilizing into the OPO signal (idler). In

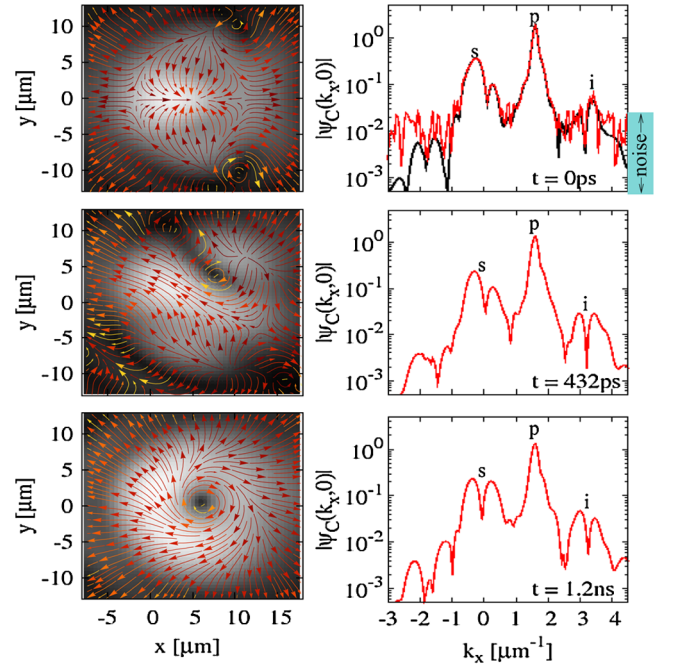


FIG. 2 (color online). Filtered signal profile $|\psi_C^s(\mathbf{r}, t)|$ with supercurrents $\nabla\phi_C^s(\mathbf{r}, t)$ (left panels) and full momentum emission $|\psi_C(k_x, 0, t)|$ (right in arbitrary units) at three different times: $t = 0$ (first row), $t = 432$ ps (second), and $t = 1.2$ ns (third)—top-hat pump with $\sigma_p = 35$ μm and $f_p = 1.12f_p^{\text{th}}$. At $t = 0$ a pulsed weak random noise of strength 0.01 (see text) is added (first row: in the right panel both OPO momentum profiles without and with the added noise are shown for comparison) and at $t = 432$ ps a vortex, with $m = -1$, enters the signal and settles into a steady state. An $m = 1$ vortex in the signal (left middle and bottom panels) and idler real space emission appears as a dip in momentum space at the signal and idler momenta (right middle and bottom panels).

the case of Fig. 2 and the right panel in Fig. 3, the noise strength is 0.01 and 432 ps after the noise pulse, a vortex with $m = -1$ ($m = +1$), enters the signal (idler) and stabilizes. Different noise strengths do not affect the final steady state but only the transient time the system needs to accommodate the vortex and reach the steady configuration. Note that parametric scattering constrains the phases of the pump, signal, and idler by $2\phi_p = \phi_s + \phi_i$. Therefore a vortex in the signal implies an antivortex in the idler and vice versa.

Furthermore, we examine whether this vortex steady state is dynamically stable by applying an additional noise pulse. For weak noise, with a strength up to 0.1, the vortex is stable and can drift around only a little before settling again into the same state. For strong noise, with strength 1 and above, the vortex gets washed away, but after a transient period the very same state enters and stabilizes again into the signal, with the possibility of flipping vorticity, as discussed later. Different noise strengths do not affect the final steady state but only the transient time.

Alternatively, one can break the $y \mapsto -y$ symmetry by a pulsed vortex probe and assess whether the stable steady

state is in any way dependent on the external perturbation. Vortices with charge $m = \pm 1$ can be generated in the OPO signal and idler, by adding a LG pulsed probe [4,15]:

$$F_{pb}(\mathbf{r}, t) = f_{pb} |\mathbf{r} - \mathbf{r}_{pb}| e^{-|\mathbf{r} - \mathbf{r}_{pb}|^2 / (2\sigma_{pb}^2)} e^{im\varphi} \times e^{i(\mathbf{k}_{pb} \cdot \mathbf{r} - \omega_{pb} t)} e^{-(t-t_{pb})^2 / (2\sigma_t^2)}, \quad (2)$$

where the probe momentum \mathbf{k}_{pb} and energy ω_{pb} are resonant with either the OPO signal or idler state. The phase φ winds from 0 to 2π around the vortex core \mathbf{r}_{pb} . Shortly after the arrival of the pulsed probe ($\sigma_t = 1$ ps), there are two possible scenarios: Either the vortex is imprinted into the signal and idler and drifts around, or no vortex gets transferred. However, the homogeneous OPO states, which are unstable towards the spontaneous formation of stable vortices following a white noise pulse, exhibit the same instability following a vortex probe pulse (see left panel in Fig. 3). The steady state vortex is independent of both the probe intensity f_{pb} and size σ_{pb} ; however, the weaker the probe, the longer the vortex takes to stabilize, between 30 and 400 ps for our system parameters. The stable vortex following the LG probe is exactly the same as the one triggered by a weak white noise (see right panel in Fig. 3), indicating that the probe acts only as a symmetry-breaking perturbation.

We can therefore infer that there are OPO conditions, such as the one in Fig. 2, where the $y \mapsto -y$ symmetric solution is dynamically unstable, and any symmetry breaking perturbation allows the signal and idler to relax into a stable steady state carrying a vortex with charge ± 1 . This suggests that such a vortex is the genuine unique OPO stable state, which, however, cannot be accessed without breaking the $y \mapsto -y$ symmetry. Instability of the uniform state to spontaneous pattern (e.g., vortex) formation is a typical feature of systems driven away from equilibrium [16]. Similarly, we find conditions for which the uniform OPO solution is unstable to spontaneous formation of a quantized vortex.

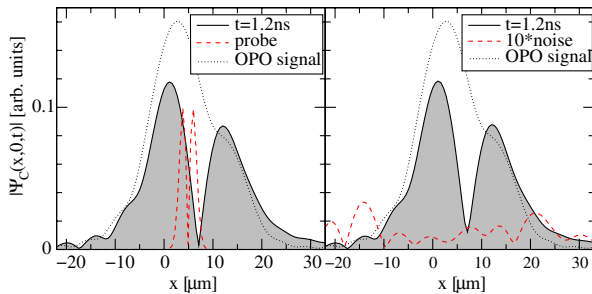


FIG. 3 (color online). Steady state filtered signal profile (dotted line) $\psi_C^2(x, 0, t)$ for $y \approx 0$ before the arrival of either a vortex probe (2) with $\sigma_{pb} \approx 1 \mu\text{m}$ (left panel, red dashed line) or a noise pulse of strength 0.01 (right panel, red dashed line)—the same OPO conditions as Fig. 2. After any perturbation breaking the $y \mapsto -y$ symmetry, the same vortex with charge $m = \pm 1$ (solid shaded curve) stabilizes into the signal.

The system symmetry can also be broken by spatial disorder. Indeed, as for nonresonantly pumped polaritons [6], we have found in our OPO simulations spontaneous stable vortices forming in a disordered landscape.

Metastability.—In addition to stable vortices, we have found OPO conditions supporting metastable vortex solutions. In this case, the symmetric OPO steady state is dynamically stable but, because of its superfluid properties, can support persistent metastable currents injected externally. Metastable solutions can be equally induced by either a vortex probe (2) or a noise pulse. However, differently from the stable case, such solutions require a threshold in the perturbation breaking the system symmetry. One example is shown in Fig. 4: The steady state shown in the second row can be triggered by adding a white noise pulse to the symmetric OPO steady state (first row in Fig. 4) only for noise strengths larger than 0.1. For weaker noises, the OPO signal is slightly perturbed and rapidly goes back to its steady state vortexless configuration. Alternatively, a vortex probe (2) can also be applied. For example, for a probe vortex with $\mathbf{r}_{pb} \approx (-6, -5) \mu\text{m}$, $\sigma_{pb} = 4.5 \mu\text{m}$, which is resonant with the OPO signal momentum and frequency, a probe intensity $f_{pb} \geq 0.45 f_p$ is required in order to generate the steady state vortex shown in the last row in the figure. Right panels in Fig. 4 show the interference fringes between the signal and the pump state, obtained by considering the full emission in space $|\psi_C(\mathbf{r}, t)|$. A vortex corresponds to a forklike dislocation in the interferences.

The spatial position of both stable and metastable steady state vortices is close to the position where the OPO signal has the currents pointing inwards (see Figs. 2 and 4). In addition, we have found that stable vortex solutions are more likely to occur in smaller pump spots such as the one in Fig. 2 rather than in larger ones, where only metastable vortex solutions can occur (see Fig. 4). Besides, we find stable vortices appearing quite close to the pump threshold. For values of κ_X and κ_C close to the experimental ones, there is only a small pump power range for stable OPO emission, above which the system tends not to reach a steady state and then starts switching off in the middle [17]. Finally, we checked that $m = \pm 1$ ($m = \mp 1$) vortex solutions can appear only into the OPO signal (idler). A vortex probe pulse of any charge m injected resonantly to the pump momentum and energy gets immediately transferred to an $m = \pm 1$ ($m = \mp 1$) vortex in the signal (idler), leaving the pump vortexless. The stability of signal $m > 1$ vortices is outside the scope of this work [18].

Conservation of charge.—When generated by a noise pulse, stable and metastable vortices have equal probability to have either charge ± 1 . Similarly, when vortices are triggered via a LG probe, their vorticity can flip during the transient period. Flipping can follow the appearance of two antivortices at the edge of the signal, one recombining with the triggered vortex. Topological charge inversion has been already predicted to occur in confined atomic Bose-Einstein condensates [19]: In the presence of an asymme-

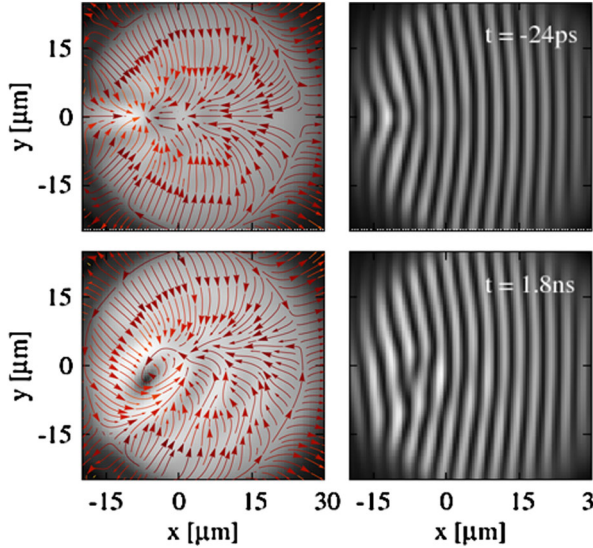


FIG. 4 (color online). Generation of an $m = +1$ metastable vortex solution into the OPO signal ($f_p = 1.24f_p^{\text{th}}$ and $\sigma_p = 70 \mu\text{m}$). First row: OPO filtered signal spatial profile together with currents (left) and interference fringes (right) are plotted at $t = -24 \text{ ps}$ before the arrival of either a strong enough vortex probe (2) or a strong enough noise pulse. The metastable vortex lasts for as long as our simulation (last row, $t = 1.8 \text{ ns}$) and requires a threshold in the intensity of the perturbation breaking the $y \mapsto -y$ symmetry.

try, breaking rotation invariance, vorticity is not a conserved quantity.

Healing length.—An approximate analytical expression for the vortex healing length can be derived for homogeneous pumping, assuming that only the signal and idler can carry angular momentum with opposite sign $\pm m$, $\psi^{s,i}(\mathbf{r}) = \sqrt{n_{s,i}} e^{i\mathbf{k}_{s,i} \cdot \mathbf{r}} e^{\pm im\varphi} \Psi^{s,i}(r)$, while the pump remains in a plane-wave state, $\psi^p(\mathbf{r}) = \sqrt{n_p} e^{i\mathbf{k}_p \cdot \mathbf{r}}$, as also supported by our numerical analysis. For pump powers close to the OPO threshold, it can be shown that signal and idler steady state spatial profiles are locked together and satisfy the following complex Gross-Pitaevskii equation:

$$\left[-\frac{1}{2m_C} \left(\frac{d^2}{dr^2} + \frac{1}{r} \frac{d}{dr} - \frac{m^2}{r^2} \right) + \alpha(\Psi^{s^2} - 1) \right] \Psi^s = 0,$$

where $|\alpha| \simeq g_X \sqrt{n_s n_i}$. This equation describes a vortex profile [11] with healing length

$$\xi = (2m_C g_X \sqrt{n_s n_i})^{-1/2}. \quad (3)$$

This expression is similar to the one of an equilibrium superfluid, with the condensate density replaced by the geometric mean of signal and idler densities. Further above threshold, the signal and idler are no longer locked together and start to develop different radii. In both the simulations in Figs. 3 and 4, we find $\xi \simeq 4 \mu\text{m}$, compatible with the estimate (3). Recently, the controlled creation of OPO

vortices by a weak continuous probe [9] has allowed us to experimentally test the validity of Eq. (3).

In conclusion, we have shown that the polariton OPO superfluid can spontaneously break the $y \mapsto -y$ system symmetry and, even in the absence of driving rotation, trapping, or disorder potential, can be unstable towards the creation of a quantized vortex state of charge ± 1 . The OPO symmetric state is generally stable; however, metastable vortices can be injected by a strong enough external probe. The size of both types of vortices is given by a healing length, which, close to threshold, is analogous to the one of equilibrium superfluids. Long-lived metastable vortices have been experimentally realized in Ref. [4], providing evidence for persistence of currents in this system. Since the parameters of our simulations are close to those of current semiconductor microcavities, the existence of stable spontaneous vortices in OPO should also be within experimental reach.

We are grateful to J.J. García-Ripoll, D. Sanvitto, J. Keeling, N.G. Berloff, and L. Viña for stimulating discussions and TCM group (Cambridge, United Kingdom) for computer resources. F.M.M. acknowledges Ramón y Cajal and INTELBIOMAT (ESF) programs. This work was supported by the Spanish MEC (MAT2008-01555, QOIT-CSD2006-00019) and CAM (S-2009/ESP-1503).

*francesca.marchetti@uam.es

†Also at London Centre for Nanotechnology, United Kingdom.

- [1] P.G. Savvidis *et al.*, *Phys. Rev. Lett.* **84**, 1547 (2000).
- [2] A. Amo *et al.*, *Nature (London)* **457**, 291 (2009).
- [3] A. Amo *et al.*, *Nature Phys.* **5**, 805 (2009).
- [4] D. Sanvitto *et al.*, *Nature Phys.* **6**, 527 (2010).
- [5] R.M. Stevenson *et al.*, *Phys. Rev. Lett.* **85**, 3680 (2000).
- [6] K.G. Lagoudakis *et al.*, *Nature Phys.* **4**, 706 (2008).
- [7] G. Nardin *et al.*, *arXiv:1001.0846*.
- [8] J. Keeling and N.G. Berloff, *Phys. Rev. Lett.* **100**, 250401 (2008).
- [9] D.N. Krizhanovskii *et al.*, *Phys. Rev. Lett.* **104**, 126402 (2010).
- [10] M. Wouters and V. Savona, *Phys. Rev. B* **81**, 054508 (2010).
- [11] L.P. Pitaevskii and S. Stringari, *Bose-Einstein Condensation* (Clarendon Press, Oxford, 2003).
- [12] D.M. Whittaker, *Phys. Status Solidi C* **2**, 733 (2005).
- [13] C. Ciuti, P. Schwendimann, and A. Quattropani, *Semicond. Sci. Technol.* **18**, S279 (2003).
- [14] D.M. Whittaker, *Phys. Rev. B* **71**, 115301 (2005).
- [15] D. Whittaker, *Superlattices Microstruct.* **41**, 297 (2007).
- [16] M.C. Cross and P.C. Hohenberg, *Rev. Mod. Phys.* **65**, 851 (1993).
- [17] D. Sanvitto *et al.*, *Phys. Rev. B* **73**, 241308 (2006).
- [18] M. Szymańska, F. Marchetti, and D. Sanvitto, *arXiv:1005.4625*.
- [19] J.J. García-Ripoll, G. Molina-Terriza, V.M. Pérez-García, and L. Torner, *Phys. Rev. Lett.* **87**, 140403 (2001).